Article

Not peer-reviewed version

Description of Kentmoseria vulgaris n. sp. (Cnidaria, Myxosporea) from Common Two-Banded Seabream Diplodus vulgaris (Sparidae), and Reclassification of Kentmoseria Lusitanica N. Comb. (Sirin et al., 2018) Based on Morphological and Molecular Data

Tiago Almeida , Luís F. Rangel , Mónica Sá , Catarina Araújo , Maria João Santos , Sónia Rocha *

Posted Date: 9 June 2025

doi: 10.20944/preprints202506.0728.v1

Keywords: myxozoa; taxonomy; bipteria; sinuolineidae; ortholineidae; morphology; phylogeny; 18S rDNA

 doi:10.20944/preprints202506.0728.v1

Article

Description of *Kentmoseria vulgaris* n. sp. (Cnidaria, Myxosporea) from Common Two-Banded Seabream *Diplodus vulgaris* (Teleostei, Sparidae), and Reclassification of *Kentmoseria lusitanica* n. comb. (Sirin et al., 2018) Based on Morphological and Molecular Data

Tiago Almeida [1], Luís F. Rangel [2,3], Mónica Sá [1,4], Catarina Araújo [2,4], Maria João Santos [2,3] and Sónia Rocha [1,4,*]

[1] School of Medicine and Biomedical Sciences (ICBAS), University of Porto, Porto, Portugal
[2] Faculty of Sciences of the University of Porto (FCUP), Porto, Portugal
[3] Interdisciplinary Centre of Marine and Environmental Research (CIIMAR), University of Porto, Matosinhos, Portugal
[4] Institute for Research and Innovation in Health (i3S), University of Porto, Porto, Portugal
* Correspondence: srrocha@icbas.up.pt

Abstract: The common two-banded seabream, *Diplodus vulgaris*, is a commercially important fish in the Mediterranean and eastern Atlantic, yet its myxosporean parasite diversity remains unknown. To address this gap, we conducted a myxosporean survey in *D. vulgaris* specimens from eastern Atlantic fishing stocks. Myxospores resembling *Kentmoseria* were observed in the urinary bladder of 3 specimens. 18S rDNA analyses, however, identified two isolates as *Bipteria lusitanica*, with the third also showing highest similarity to this species. Morphological comparison revealed significant overlap between *B. lusitanica* and *Kentmoseria*, particularly in the suture line orientation. Accordingly, we reclassify *B. lusitanica* as *Kentmoseria lusitanica* n. comb. and describe a novel species, *Kentmoseria vulgaris* n. sp. The unclear boundaries between *Bipteria* and *Kentmoseria* are highlighted, though redefining or suppressing either genus remains premature without sequencing their type species. Moreover, our phylogenetic analyses show these species clustering among Sinuolineidae, rather Ortholineidae, supporting the dismantling of Ortholineidae and placement of *Kentmoseria* within Sinuolineidae. The ancestral placement of *Bipteria vetusta* suggests it is taxonomically distinct and not a member of the Sinuolineidae. Finally, the occurrence of two *Kentmoseria* spp. in *D. vulgaris* suggests diversification in *Diplodus*, underscoring the need to study myxosporean diversity in wild stocks to assess aquaculture risks.

Keywords: myxozoa; taxonomy; *Bipteria*; sinuolineidae; ortholineidae; morphology; phylogeny; 18S rDNA

1. Introduction

Myxosporeans (Class Myxozoa, subclass Myxosporea) are obligatory cnidarian parasites with a complex life cycle that usually involves fish as intermediate hosts [1,2]. Myxospores are produced in the fish and, when released into the water, infect susceptible annelid worms. In these hosts, parasites develop into actinospores that emerge to infect fish [3]. Many myxosporeans cause serious diseases linked to morbidity and mortality in wild and farmed fish populations, adversely affecting fisheries and aquaculture industries [4]. Despite the description of more than 2,600 species worldwide,

 doi:10.20944/preprints202506.0728.v1

distributed across 64 genera and 17 families [5], it is widely acknowledged that the true diversity of these parasites is overly underestimated [6].

Myxospore morphological features, vertebrate host, and tissue specificity have traditionally served as key taxonomic criteria for distinguishing among myxosporean orders, suborders, families, and genera [2]. At the level of orders and suborders, classification is primarily based on the number and arrangement of shell valves and the number and orientation of polar capsules relative to the sutural plane. In turn, characteristics such as the presence or absence of caudal appendages and the shape of the suture line are more informative at the family and genus levels [2,5]. Nonetheless, molecular studies have shown that myxosporean phylogenetic relationships are not consistent with a taxonomic approach based on myxospore morphology [1,7–12].

The family Ortholineidae of the suborder Variisporina is characterized by spherical to irregularly ellipsoidal myxospores that are bilaterally symmetrical along a straight suture line, with two anteriorly located polar capsules shifted sidewise in the sutural plane [2]. This family was originally erected to accommodate the genera *Ortholinea* and *Neomyxobolus*, which develop in the urinary tract of marine and freshwater fishes [13]. The genera *Cardimyxobolus*, *Triangula*, and *Kentmoseria* Lom and Dyková, 1995 were added later, despite the first two being histozoic in several organs [2]. The genus *Kentmoseria*, in particular, is defined by the features of its type- and only species, *K. alata* (Kent and Moser, 1990), a coelozoic parasite in the urinary tract of the marine fish *Chaetodon rainfordi* McCulloch, 1923 from the Great Barrier Reef off Australia [14]. Myxospores of *Kentmoseria* are elongated, wider anteriorly than posteriorly, slightly flattened parallel to the straight suture, and presenting pointed valvular projections that extend backwards from the posterior half of the smooth shell valves. Two pyriform polar capsules are located anteriorly and open laterally [2,14].

Also within the Variisporina, the family Sinuolineidae Shulman, 1959 comprises species that are also mostly coelozoic in the urinary system of marine fish [15], but whose myxospores are spherical or inversely pyramidal, may present caudal or lateral projections, and have two polar capsules located anteriorly, spaced apart, and perpendicular to the sinuous suture line [2]. Within this family, the genus *Bipteria* Kovaleva, Zubchenko and Krasin, 1983 is characterized by the inversely pyramidal shape of its myxospores in the sutural plane, with a pointed end extending backwards, and a curved sutural line. The anterior end of each shell valve extends into a wing-like projection containing parts of the valvogenic nucleus, and the polar capsules are spherical, opening to opposite sides of the myxospore. In transverse section, the myxospores are ellipsoid [16]. This genus presently comprises eight species that either infect the excretory system or the gallbladder of their fish hosts [2,17]. The type species, *Bipteria admiranda* Kovaleva, Zubchenko and Krasin, 1983 parasitizes the urinary system of *Pagellus acarne* (Risso, 1827). Congruently, *Bipteria magna* Kovaleva, Zubchenko and Krasin, 1983 and *Bipteria minima* Kovaleva, Zubchenko and Krasin, 1983 in *Albatrossia pectoralis* (Gilbert, 1892), and *Bipteria lusitanica* Sirin, Santos and Rangel, 2018 in *Diplodus sargus* (Linnaeus, 1758) all parasitize the urinary bladder of their hosts; while *Bipteria nototheniae* Kovaleva and Rodyuk, 1991 infects the renal tubules of *Patagonotothen ramsayi* (Regan, 1913). *Bipteria indica* Kalavati and Anuradha, 1995 in *Mugil cephalus* Linnaeus, 1758, *Bipteria merluccii* Kovaleva, Velev and Vladov, 1993 in *Merluccius polli* Cadenat, 1950, and *Bipteria vetusta* Kodádková et al., 2015 in *Chimaera monstrosa* Linnaeus, 1758 are gallbladder parasites [16–21]. Following the reclassification of *Bipteria formosa* within the genus *Sphaerospora* [11], *B. vetusta* and *B. lusitanica* are the only *Bipteria* species with molecular data available. These have been recognized to cluster widely apart from each other in phylogenetic analyses [17,20].

Common two-banded seabream *Diplodus vulgaris* (Geoffroy Saint-Hilaire, 1817) of the family Sparidae Rafinesque, 1818 is a commercially important fish native to the Mediterranean and eastern Atlantic region [22]. According to the most recent capture records, a total of 687.58 tonnes in live weight were captured in 2022, with notable contributions from Portugal and Spain, corresponding to 267.26 and 213.80 tonnes, respectively [23]. Efforts have been made by Italy and Turkey to cultivate this species in aquaculture, reflecting a growing interest in the sector [24].

Despite the economic relevance of *D. vulgaris*, there is no information about myxosporean infections in this fish. In fact, few myxosporean surveys have been performed on Diplodus fish [25–

 doi:10.20944/preprints202506.0728.v1

30]. In Portugal, only white seabream *D. sargus* (Linnaeus, 1758) has been examined for myxosporean infections, hosting *B. lusitanica* in the interstitial tissue of the kidney and in the urinary bladder [20], and Ceratomyxa sargus Rocha et al., 2023 and *Zschokkella auratis* Rocha et al., 2013 in the gallbladder [31,32]. Thus, the present study aimed to provide data on the diversity of myxosporean parasites infecting commercial stocks of common two-banded seabream *D. vulgaris*, through combined microscopic and molecular methodologies.

2. Materials and Methods

2.1. Fish Sampling and Myxosporean Survey

In December 2022, 12 specimens of common two-banded seabream *Diplodus vulgaris* (Geoffroy Saint-Hilaire, 1817) caught off the Portuguese Northern Atlantic coast were purchased from a fish auction in the city of Aveiro (40° 38' 39.37" N, -8° 38' 43.94" W), Portugal. Following transport to the laboratory on ice, specimens were examined for detecting myxosporean developmental stages in external (gills, fins, eyes, and skin) and internal (brain, gallbladder, gonads, heart, intestines, kidney, liver, muscle, spleen, stomach, swim and urinary bladder) organs. Fresh tissue smears were analysed and photographed using a Zeiss Axiophot microscope (GrupoTaper, Sintra, Portugal) equipped with a Zeiss Axiocam ICC3 digital camera. Axiovision 4.6 Software was used for image analysis. The dimensions of fresh mature myxospores were determined using ImageJ, following the guidelines by Lom and Arthur [33]. All measurements are given in micrometres (μm), and include mean ± standard deviation, range of variation, and number of myxospores measured (n).

2.2. DNA Extraction, Amplification, and Sequencing

Infected tissue samples were preserved in absolute ethanol at 4 ºC. DNA was extracted with the GenEluteTM Mammalian Genomic DNA Miniprep Kit (Sigma-Aldrich, St. Louis, USA) following the manufacturers guidelines, and stored at -20 ºC until further use.

Amplification of the myxosporean 18S ribosomal DNA (18S rDNA) sequence was targeted using a nested PCR. Both first and second round PCRs were performed in 50 μL reactions containing 5 μL of 10x reaction buffer for Supreme NZYTaq II DNA polymerase (NZYTech, Lisbon, Portugal), 2.5 mM of MgCl2, 10 nmol of dNTP (NZYTech, Lisbon, Portugal), 10 pmol of each primer, 1.5 units of Supreme NZYTaq II DNA polymerase (NZYTech, Lisbon, Portugal), and approximately 100–150 ng of genomic DNA, made up to the final volume with ultrapure sterilized water. In the first round of the nested PCRs, the universal primers ERIB1 and ERIB10 were used, with cycling conditions as follows: initial denaturation at 95 ºC for 3 min; 30 cycles at 95 ºC for 1 min, 48 ºC for 1 min, and 72 ºC for 1 min 45 s; and final extension at 72 ºC for 10 min. For the second round of the nested PCRs, other eukaryotic-universal and myxosporean specific primers were used (Table 1), employing the following cycling conditions: initial denaturation at 95 ºC for 3 min; 35 cycles at 95 ºC for 45 s, 53 ºC for 45 s, and 72 ºC for 1 min 30 s; and final extension at 72 ºC for 7 min. Reactions were run on a Hybaid PxE Thermocycler (Thermo Electron Corporation, Milford, MA, USA). Electrophoresis of the PCR products was performed in a 1% agarose 1× Tris - acetate - EDTA buffer gel stained with GreenSafe Premium (NZYTech, Lisbon, Portugal). Positive amplicons were purified using the ExoFast method [39] and sequenced directly by Stabvida (Oeiras, Portugal).

 doi:10.20944/preprints202506.0728.v1

Table 1. Primers used for amplification of the 18 rDNA.

Name	Sequence (5′-3′)	Paired with	Source
ERIB1	ACC TGG TTG ATC CTG CCA G	ERIB10	Barta et al. (1997)
ERIB10	CTT CCG CAG GTT CAC CTA CGG	ERIB1	Barta et al. (1997)
18E	CTG GTT GAT CCT GCC AGT	ACT1R, MyxGen4r	Hillis and Dixon (1991)
MyxospecF	TTC TGC CCT ATC AAC TTG TTG	MyxGen4r, 18R	Fiala (2006)
ACT1R	AAT TTC ACC TCT CGC TGC CA	18E	Hallett and Diamant (2001)
MyxGen4r	ACC TGT TAT TGC CAC GCT	18E, MyxospecF	Kent et al. (2000)
18R	CTA CGG AAA CCT TGT TAC G	MyxospecF	Whipps et al. 2003

2.3. Sequence Assembly and Phylogenetic Analysis

A consensus 18S rDNA sequence of each isolate was assembled by aligning corresponding forward and reverse sequence segments using ClustalW in MEGA 11 [40]. Assembled sequences were submitted to Basic Local Alignment Search Tool (BLASTn) for determining closest relatives in the National Centre for Biotechnology Information database. These were included in the 18S rDNA dataset generated for phylogenetic analyses and corresponded to marine urinary bladder and gallbladder species, including *B. lusitanica* (MF538777). The 18S rDNA sequences of *B. vetusta* (KM267557) and other representatives of the polychaete-infecting (marine) lineage were also added to the dataset, as were a few species of the oligochaete-infecting (freshwater) lineage to be used as outgroup. Alignments were performed using the E-INS-i refinement method in MAFFT version 7 [41] available online, and ambiguous characters were removed using Gblocks v0.91b with less stringent parameters [42,43]. Maximum likelihood (ML) was performed using the general time reversible (GTR) model chosen based on the lowest score of the Bayesian information criterion and corrected Akaike information criterion. The analysis was run on the PhyML 3.0 program [42,44] available at https://www.phylogeny.fr/, with bootstrap confidence values calculated from 1,000 replicates. Bayesian inference (BI) analysis was performed in MrBayes v.3.2.6 [45], with the GTR model with gamma-shaped rate variations across sites (Invgamma) (GTR + I + G). Posterior probabilities were determined using the Markov chain Monte Carlo method, with 4 chains running simultaneously for 1 million generations, burn-in set at 25% and trees sampled every 500 generations.

3. Results

The microscopic survey conducted in this study allowed the detection of myxosporean infections in several organs of *D. vulgaris*, in which myxospores were observed within plasmodia or isolated. Of the 12 specimens examined, 10 were infected by this parasite group, resulting in an overall prevalence of infection of 83.3%. Although a broad parasitological study was not conducted, three individuals were also noted to be parasitized by tongue-eating lice (Crustacea, Cymothoidae).

Infection by myxospores resembling the *Kentmoseria* morphotype was detected in the urinary bladder and kidney interstitial tissue of three specimens (specimens #3, 4 and 9; Table 2). Cysts of *Sphaerospora* also occurred in the kidney of four specimens (specimens #4, 5, 7 and 11; Table 2), while *Myxobolus* myxospores appeared dispersed in both the kidney and spleen tissues (specimens #1, 2, 6 and 7; Table 2). Kidney co-infections were detected in two individuals: specimen #4 displayed both *Kentmoseria* and *Sphaerospora* myxospores, and specimen #7 showed *Myxobolus* and *Sphaerospora* myxospores (Table 2). Two *Ceratomyxa* morphotypes were observed in the gallbladder of a single

 doi:10.20944/preprints202506.0728.v1

individual (specimen #12; Table 2). This study focuses on the description of the *Kentmoseria* isolates; the other isolates will be reported elsewhere.

Table 2. Myxosporean infection in the organs of the 12 specimens of *Diplodus vulgaris* examined, as determined by light microscopic observations. Kv *Kentmoseria vulgaris* n. sp.; Kl *Kentmoseria lusitanica* n. comb.; Sp *Sphaerospora* sp.; Mb *Myxobolus* sp.; C1 *Ceratomyxa* sp. 1; C2 *Ceratomyxa* sp. 2.

	D. vulgaris specimen #											
	1	2	3	4	5	6	7	8	9	10	11	12
Gallbladder	–	–	–	–	–	–	–	–	–	–	–	C1, C2
Spleen	Mb	Mb	–	–	–	Mb	–	–	–	–	–	–
Kidney	Mb	–	Kl	Sp, Kl	Sp	Mb	Mb, Sp	–	Kv	–	Sp	–
Urinary bladder	–	–	Kl	Kl	–	–	–	–	Kv	–	–	–

Morphological analyses revealed the presence of two distinct *Kentmoseria* isolates in infected urinary bladder and kidney samples. Congruently, BLASTn search matched the isolates in specimens #3 and #4 to the 18S rDNA sequence of *B. lusitanica* (MF538777) but retrieved no significant similarity for the isolate infecting specimen #9. Thus, based on morphological and molecular data, the latter is herein described as a novel species, *Kentmoseria vulgaris* n. sp.

3.1. Species Characterisation of Kentmoseria vulgaris n. sp.

Light microscopy: Disporic plasmodia subspherical, 15.2 ± 1.2 (14.4–16.1) long and 13.9 ± 1.0 (13.2–14.6) wide (n = 2) (Figure 1A), and mature myxospores floating free in the urine (Figure 1B-I). Myxospores also observed dispersed in the interstitial tissue of the kidney. Mature myxospores triangular to inverse pyramidal in valvular view and ellipsoidal in sutural view, measuring 12.6 ± 0.9 (10.5–14.0) in length (n = 28), 9.7 ± 0.7 (8.6–10.8) in width (n = 11), and 9.1 ± 0.5 (8.3–10.0) in thickness (n = 12) (Figure 1B, C). Myxospores formed by two symmetric smooth valves united along a prominent and apparently straight suture line (Figure 1D). Each valve with a wing-like projection forming in the myxospore anterior end and extending beyond its posterior end (Figure 1E-G). Wing-like projections 16. 9 ± 1.2 (15.3–19.1) long (n = 21), each displaying a valvogenic nucleus located near the myxospore posterior end (Figure 1H). Two subspherical polar capsules, 4.1 ± 0.2 (3.7–4.7) long and 3.8 ± 0.3 (3.4–4.3) wide (n = 20), symmetric, located at the same level at the anterior end, and opening to opposite sides (Figure 1B, I). Polar tubule coiled in 5 turns (Figure 1I). Schematic drawings depicting the myxospores in valvular and sutural view are provided in Figure 2.

Sites of infection: Urinary bladder and kidney interstitial tissue.

Type locality: Portuguese Atlantic coast off the city of Aveiro (40° 38' 39.37" N, -8° 38' 43.94" W).

Prevalence of infection: 1 infected out of 12 individuals examined (8.3%).

Material deposited: Series of phototypes of the hapantotype deposited together with a representative DNA sample in the Natural History and Science Museum of the University of Porto, Portugal, reference CIIMAR ####.##.

Etymology: The specific epithet "*vulgaris*" refers to the host species name.

Molecular data: 18S rDNA sequence with 1,925 bp (GenBank accession number PV617282).

Remarks: Comparison with *K. alata* revealed some morphometric similarities in myxospore dimensions. However, the polar capsules of *K. vulgaris* n. sp. are subspherical instead of spherical, and overall smaller. Additionally, these species differ in host specificity and geographic distribution [14]. *Kentmoseria alata* was reported to infect *Chaetodon rainfordi* McCulloch, 1923 (Chaetodontidae), a species restricted to the Great Barrier Reef, adjacent coastal areas, and Lord Howe Island [46]. In contrast, the host of *K. vulgaris* n. sp. is distributed along the Eastern Atlantic [47].

No significant morphological or morphometric similarities were observed with *Bipteria* spp. [16–21], primarily because *Bipteria* myxospores are inversely pyramidal in the sutural plane, unlike those

 doi:10.20944/preprints202506.0728.v1

of *Kentmoseria*, which are inversely pyramidal in the valvular plane [2]. *Bipteria lusitanica* is a notable exception, possessing myxospores that are inversely pyramidal in the valvular plane. Although being morphologically similar to *B. lusitanica* and sharing the same host and tissue tropism [20], *K. vulgaris* n. sp. myxospores are overall smaller with subspherical polar capsules, instead of spherical polar capsules. In addition, the 18S rDNA sequence of *K. vulgaris* n. sp. differs from that of *B. lusitanica* (MF538777) by 7.6%, despite it being the closest match in the BLASTn search; all other hits showed genetic divergences greater than 15.0%.

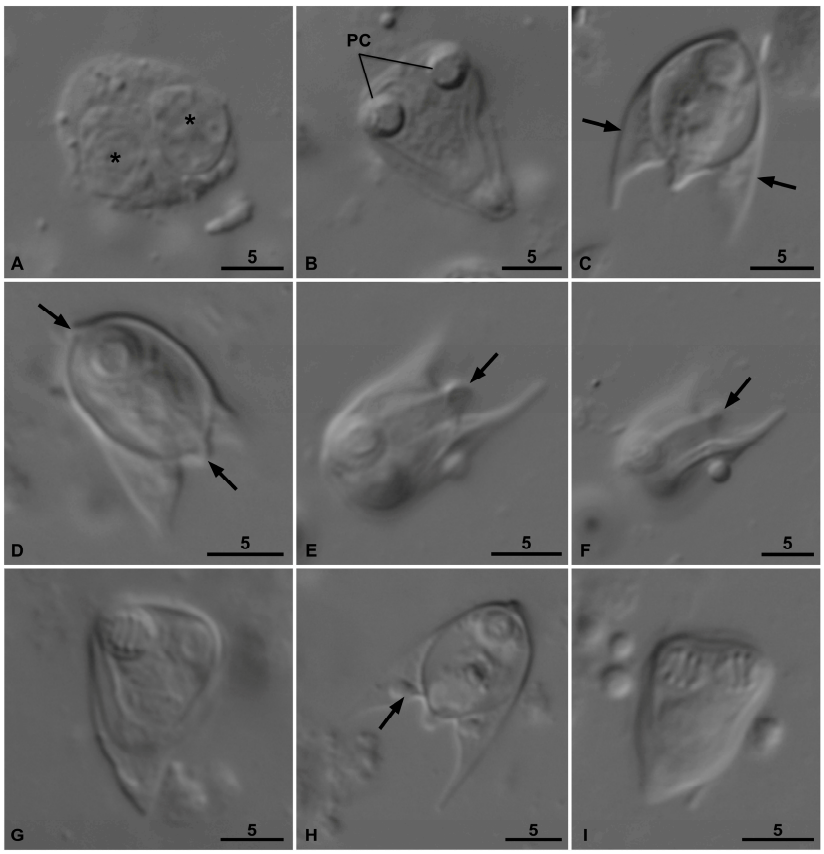

Figure 1. Light micrographs of Kentmoseria vulgaris n. sp. (**A**) Disporic plasmodium evidencing two developing sporoblasts (*); (**B**) Myxospore inversely pyramidal in valvular view, with two polar capsules (PC) opening to opposite sides at the anterior end; (**C**) Myxospore ellipsoidal in sutural view, sowing each valve bearing a wing-like projection that extends from the posterior end (arrows); (**D**) Myxospore evidencing the straight suture line (arrows) uniting the valves; (**E, F**) Myxospore in sutural view evidencing the wing-like projections forming at the anterior end. These projections run the myxospore length and extend from its posterior end. Notice the suture line (arrow). (**G**) Myxospore evidencing the appearance of the wing-like projections in valvular view. (**H**) A large valvogenic nucleus (arrow) was observed at the anterior portion of each wing-like projection; (**I**) Valvular view showing the two subspherical polar capsules positioned anteriorly and opening to opposite sides, each containing a coiled polar tubule. Scales in μm.

 doi:10.20944/preprints202506.0728.v1

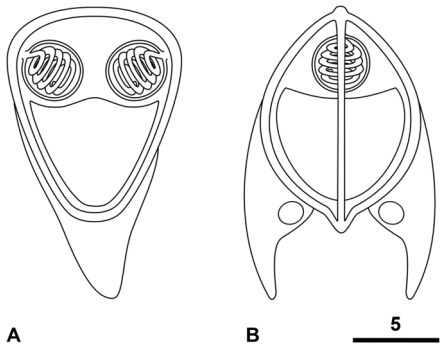

Figure 2. Schematic drawing of Kentmoseria vulgaris n. sp. myxospores in valvular view (**A**) and sutural view (**B**). Scales in µm.

3.2. Kentmoseria lusitanica n. comb. (Sirin, Santos and Rangel, 2018)

Two out of the 12 specimens analyzed (16.7%) presented infection by this species, which was co-infective with an unidentified *Sphaerospora* sp. in the kidney of specimen #4. Co-infection with *Kentmoseria vulgaris* n. sp. was not detected either microscopically or molecularly. Species identification was based on myxospore morphometry, organ of infection, and molecular data of the 18S rDNA. Myxospores were triangular to inverse pyramidal in valvular view, measuring 11.7 ± 0.8 (10.6–13.1) in length and 13.5 ± 0.9 (11.9–14.7) in width (n = 13). In sutural view, myxospores were ellipsoidal, measuring 10.7 in thickness (n = 1). Myxospore wall composed of two smooth valves, each bearing a wing-like projection, 15.1 ± 1.5 (12.8–16.6) long (n = 7). These formed at the anterior end of the myxospores but extended beyond its posterior end. Two symmetrical subspherical polar capsules, 4.1 ± 0.3 (3.7–4.6) long and 3.8 ± 0.2 (3.5–4.3) wide (n = 12), were located at the same level at the anterior end and opened to opposite sides. The number of polar tubule coils could not be determined (Figure 3).

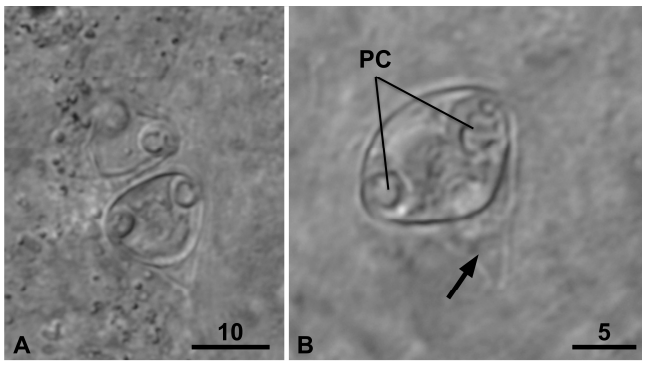

Figure 3. Light micrographs of Kentmoseria lusitanica n. comb. (**A, B**) Myxospores in valvular view, inversely pyramidal, with two polar capsules (PC) widely set apart and opening to opposite sides at the anterior end. Notice the wing-like projections (arrow) covering the valves and extending from the myxospore posterior end.

These morphological and morphometric features somewhat differ from those reported in the species original description, namely in terms of myxospore width range [13.5 ± 0.9 (11.9–14.7) vs 11.6 ± 0.4 (10.9–12.3)] and polar capsule shape and size [pyriform, 4.1 ± 0.3 (3.7–4.6) x 3.8 ± 0.2 (3.5–4.3) vs spherical, 4.4 ± 0.2 (4.1–5.0)] [20]. Potential differences in myxospore thickness could not be evaluated given that this morphometric parameter was obtained from a single myxospore in our study. Despite these morphological differences, the partial 18S rDNA sequence obtained from the isolate in the urinary bladder of specimen #3 comprised 1,452 bp that were identical to the sequence of *K. lusitanica* (MF538777) obtained from urinary bladder infections in white seabream *D. sargus*, previously captured from the same geographical location [20].

 doi:10.20944/preprints202506.0728.v1

3.3. Phylogenetic Analysis

ML and BI phylogenetic analyses resulted in overall similar tree topologies (Figure 4). The 18S rDNA sequences of *K. vulgaris* n. sp. and *K. lusitanica* n. comb. cluster together within the well-supported urinary clade of the polychaete-infecting (marine). The urinary clade is highly heterogeneous, encompassing not only other species of the family Sinuolineidae, such as *Latyspora*, *Sinuolinea*, *Schulmania*, but also species of the families Parvicapsulidae (*Parvicapsula*) and Myxidiidae (*Zschokkella*). *Bipteria vetusta* clusters distantly from its congeners, being positioned at the basis of the polychaete-infecting (marine) lineage.

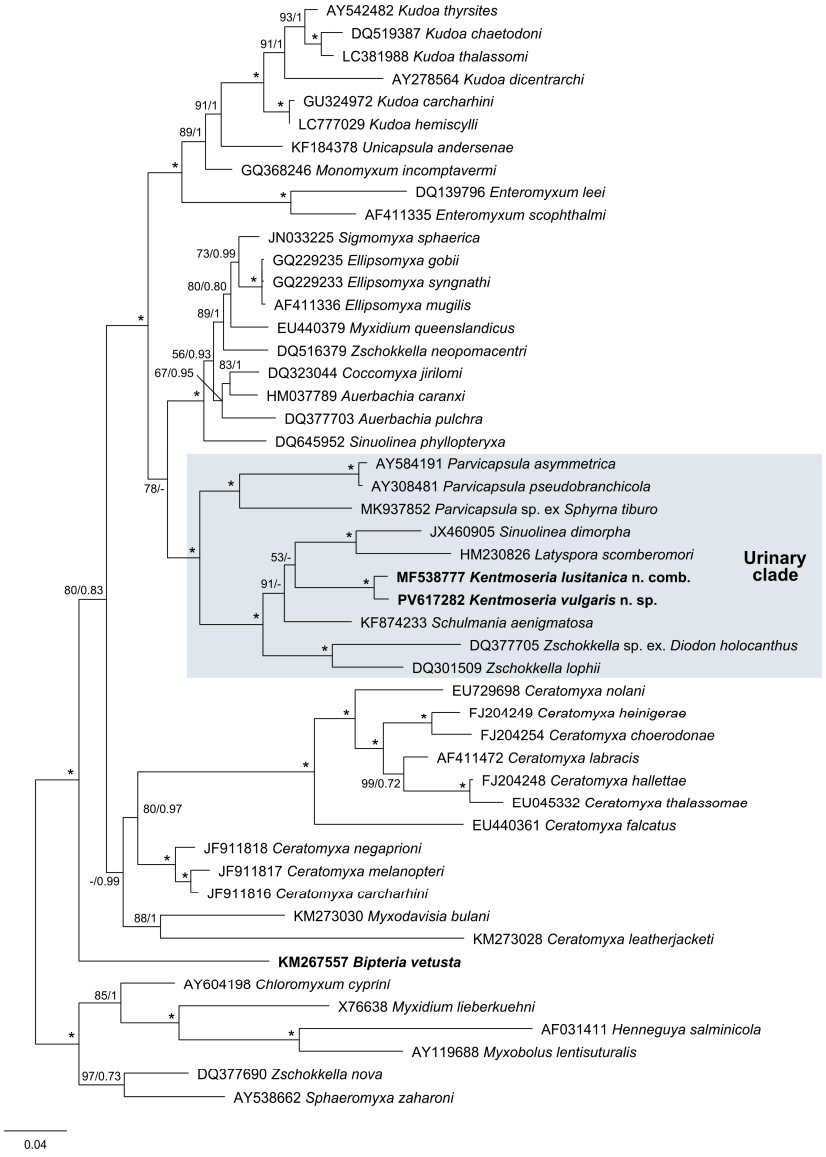

Figure 4. Maximum likelihood tree topology of the 18S rDNA of Kentmoseria species and other representatives of the polychaete-infecting (marine) lineage. Support values at branching points are ML bootstrap values/ BI probabilities; asterisks indicate full support in both methodologies; dashes are shown for values less than 50%. The sequences of Kentmoseria spp. and Bipteria vetusta are indicated in bold. .

4. Discussion

The present study describes a novel myxosporean parasite found infecting the urinary bladder and kidney interstitial tissue of common seabream *D. vulgaris*. The taxonomic assignment of this species based on myxospore morphology and molecular data proved challenging. This highlights the absence of consistent morphological boundaries between distinct myxosporean genera and

 doi:10.20944/preprints202506.0728.v1

underscores discrepancies between phylogenetic relationships and traditional taxonomy based solely on myxospore morphology [1,7–12]. In fact, several myxosporean genera are known to have convergent morphotypes that hinder correct identification of known and new species, e.g. *Ellipsomyxa*, *Myxidium*, *Zschokkella*, and *Sigmomyxa* [5,7,8,10,31,48,49]. Following the implementation of molecular tools, numerous taxonomic revisions have been performed in the past few decades to resolve poly- or paraphyletic taxa. For instance, the families Pentacapsulidae, Hexacapsulidae, and Septemcapsulidae were suppressed and their genera synonymized with *Kudoa* of the family Kudoidae, based on molecular evidence that the number of polar capsules constituted an artificial criterion for discriminating between these families [12]. The genus *Polysporoplasma* was suppressed due to clustering of its type species within the *Sphaerospora sensu stricto* lineage [11], as was the genus *Leptotheca*, which members were synonymized with *Ceratomyxa* and *Sphaerospora* [50]. In the other way around, the family Myxobilatidae was resurrected to encompass the genera *Acauda*, *Hoferellus*, and *Myxobilatus*, formerly ranked within different families [51]. Several new genera have also been erected to incorporate species that, whilst being morphologically similar to the morphotypes of other genera, can be differentiated based on phylogenetic and biological data, e.g. *Ceratonova* and *Paramyxidium* [52,53]. Despite these advances, many myxozoan taxa remain poly- or paraphyletic, a situation that may progressively change by the exponential increase of available molecular data.

The myxospores analysed in this study were triangular to inversely pyramidal in valvular view, with each valve bearing a wing-like projection originating at the anterior end and extending beyond the posterior extremity of the myxospore. This configuration is largely consistent with the diagnostic features of the genus *Kentmoseria* [2,54], particularly with respect to myxospore shape and the position of the suture line relative to the plane of the polar capsules. It differs in the morphology of the valve projections, which in *Kentmoseria* are described as extending backwards from the posterior half of the valves. In accordance with this definition, the schematic illustration of the type and only known species, *K. alata*, shows valve projections arising from the posterior half of the myxospore [14].

However, it is important to note that the study by Kent and Moser [14] includes only two low-quality myxospore photographs, limiting the ability to fully assess morphological features. Similarly, in the present study, several light microscopy images failed to clearly depict the anterior origin of the valve projections, which could have hindered accurate morphological characterization. Furthermore, the site of infection and host type of the isolates analysed are consistent with those described for *Kentmoseria*, as members of this genus are coelozoic parasites of the urinary tract in marine fishes [2,54]. Based on the combined morphological and biological data, the myxosporean isolates recovered from the urinary bladder of *D. vulgaris* can therefore be tentatively assigned to the genus *Kentmoseria*.

Molecular analyses revealed that the 18S rDNA sequences of the urinary bladder isolates from specimens #3 and #4 were identical to that of *B. lusitanica* (MF538777). The isolate from specimen #9 also exhibited the highest similarity (92.4%) to this species. Morphometric comparison between the isolates from specimens #3 and #4 and *B. lusitanica* original description from *D. sargus* revealed several significant morphometric differences indicative of intraspecific morphological variability. This is not rare among myxosporeans and usually correlates with adaptation to different hosts [55,56]. Examination of *B. lusitanica* myxospores – both from our observations and from light microscopy images and schematic illustrations in the original species description by Sirin et al. [20] – further revealed notable morphological similarities with *K. vulgaris* n. sp., particularly regarding the position of the suture line, which lies parallel to the plane of the polar capsules. This contrasts with the defining morphological characteristics of the genus *Bipteria*, whose myxospores are triangular to inversely pyramidal in the sutural plane, meaning the suture line is oriented perpendicular to the plane of the polar capsules [2].

In light of these findings, we propose the reclassification of *B. lusitanica* as *Kentmoseria lusitanica* n. comb. Although the suture line of this species was described as curved at the myxospore apex [20], rather than straight as in *Kentmoseria* [2,54], this feature may have been overlooked in *K. alata* and *K. vulgaris* n. sp. due to the difficulty of obtaining apical views of the myxospores. Nevertheless, in all three species, the suture line appears straight when viewed laterally (i.e., in sutural view). It is

 doi:10.20944/preprints202506.0728.v1

therefore plausible that the suture line in *Kentmoseria* is slightly curved apically but appears straight in lateral view.

Regarding potential broader taxonomic implications, our findings highlight the tenuous distinction between the genera *Bipteria* and *Kentmoseria*, especially considering that the original description of the former only states that the suture line is sinuous, without specifying its position relative to the polar capsules plane [16]. Morphological similarities between the two genera were inclusively observed by Lom and Dyková [54], who noted that *K. alata* valve projections resembled those of the *Bipteria* type species – *B. admiranda*. These authors established the genus *Kentmoseria* to accommodate *K. alata*, which was originally classified within *Ortholinea*, but differed from other members of that genus by having valvular projections. It can be inferred that the initial classification of *K. alata* influenced the establishment of *Kentmoseria* within the family Ortholineidae of the suborder Platysporina, despite its notable morphological resemblance to *Bipteria*, a genus within the suborder Variisporina. Thus, it is conceivable that these genera may eventually be synonymized, pending availability of molecular data from their respective type species. Until such data are obtained, it remains premature to propose the suppression of *Kentmoseria* or to revise the definition of *Bipteria*, as this could exacerbate existing inconsistencies between myxozoan taxonomy and phylogeny.

This study provides the first molecular data for the genus *Kentmoseria*. Our phylogenetic analyses show that *K. vulgaris* n. sp. and *K. lusitanica* n. comb. cluster together among species from the family Sinuolineidae, namely *Sinuolinea*, *Latyspora*, and *Schulmania*, rather than with other members of the family Ortholineidae. Previously published cladograms have consistently placed genera from Ortholineidae within other myxozoan families. The few available sequences of *Triangula* and *Cardimyxobolus* cluster within the Myxobolidae [10,57–59], while *Ortholinea* are positioned among the Myxobilatidae [57,60–64]. No molecular data are currently available for *Neomyxobolus*. Based on these observations, Karlsbakk et al. [57] proposed dismantling the family Ortholineidae, with *Ortholinea* transferred to Myxobilatidae, and *Cardimyxobolus*, *Neomyxobolus* and *Triangula* moved to the suborder Platysporina but kept as *incertae sedis* pending sequencing of their type species. In their proposal, *Kentmoseria* was retained in the suborder Variisporina within the family Sinuolineidae. Although this taxonomic setting has not been broadly adopted by taxonomists, our findings strengthen the notion that the family Ortholineidae is not supported by phylogenetic analyses, reinforcing the placement of the genus *Kentmoseria* within Sinuolineidae, as previously suggested by Karlsbakk et al. [57].

Following the taxonomic reclassification of *K. lusitanica* n. comb., *B. vetusta* remains the sole species within the genus with available molecular data. Phylogenetic analyses have shown that this species clusters distantly from the Sinuolineidae and occupies the most basal position within the polychaete-infecting (marine) lineage, followed by *Ceratomyxa* [17,20]. This basal placement, coupled with morphological and tissue tropism similarities to *Ceratomyxa*, has been interpreted as indicative of a close evolutionary relationship between *B. vetusta* and *Ceratomyxa*, supporting the evolutionary ancestry of the *Ceratomyxa* morphotype [17]. In our view, this phylogenetic framework does not support *B. vetusta* as a member of the Sinuolineidae. It further suggests its taxonomic distinction from other genera for which molecular data exist.

Bipteria vetusta was described from a holocephalan host (Chondrichthyes), which evolutionary analyses reveal to be more ancient hosts of myxozoans than Teleostei [8,17,65–67]. Acknowledging this ancestral relationship, it is unlikely that future sequencing of other gallbladder-infecting *Bipteria* species will place them within the same clade as *B. vetusta*. As parasites of teleost hosts, *B. indica* and *B. merluccii* are expected to follow the general trend of myxosporeans to cluster based on tissue tropism [7,8,17,68], and group among other gallbladder-infecting species – likely within the *Ceratomyxa* clade, as previously proposed [17]. This hypothesis is further supported by previous findings of other *Ceratomyxa*-like, gallbladder-infecting myxosporeans with wing-like appendages, such as *Pseudalatospora kovalevae* Kalavati et al., 2013 and *Palliatus indecorus* Schulman et al., 1979, as members of the *Ceratomyxa* clade [7,9,69]. These issues emphasize the need to sequence more urinary

 doi:10.20944/preprints202506.0728.v1

system-infecting myxosporean species to improve our understanding of the evolutionary trajectories of these parasites.

Overall, our findings show that morphological boundaries between *Bipteria* and other myxosporean genera are poorly defined. A similar conclusion was reached by Bartošová et al. [11], who reclassified *Sphaerospora formosa* (Kovaleva and Gaevskaya, 1979) based on congruent morphological and molecular evidence. Accordingly, we anticipate that the continued acquisition of molecular data from *Bipteria*, namely from its type species, will prompt further taxonomic revisions, which are crucial for aligning myxosporean taxonomy with phylogenetic data.

Still regarding our phylogenetic analysis, the placement of *K. vulgaris* n. sp. and K. lusitanica n. comb. within the highly heterogenous marine urinary bladder clade reinforces the importance of tissue tropism as a key evolutionary character, essential for understanding host-parasite evolutionary interactions [7,8,68]. The occurrence of two closely related *Kentmoseria* congeners in *D. vulgaris* and *D. sargus* further suggests significant coevolution and diversification of this myxosporean genus in *Diplodus* fish, and potentially among sparids in general, considering that *B. admiranda* was described parasitizing axillary seabream *P. acarne* (Sparidae) [16].

The detection of multiple myxosporeans in *D. vulgaris* underscores the importance of studying parasite biodiversity in this fish population within its natural environment, which would ultimately contribute to a better understanding of the potential risks to aquaculture.

Author Contributions: Conceptualization, S.R.; Validation, S.R.; Formal Analysis, T.A., LF.R. and S.R.; Investigation, T.A., M.S., L.F.R., C.A. and S.R.; Resources, S.R. and M.J; Data Curation, S.R.; Writing – Original Draft Preparation, T.A.; Writing – Review & Editing, S.R. and M.S.; Visualization, T.A., M.S., L.F.R., C.A., M.J.S. and S.R.; Supervision, S.R.; Project Administration, S.R.; Funding Acquisition, S.R.

Funding: This research was funded by national funds through FCT – Foundation for Science and Technology: S.R., project PTDC/BIA-BMA/6363/2020 (http://doi.org/10.54499/PTDC/BIA-BMA/6363/2020) and employment contract 2022.06670.CEECIND/CP1735/CT0007 (https://doi.org/10.54499/2022.06670.CEECIND/CP1735/CT0007); L.F.R., employment contract CEECIND/03501/2017/CP1420/CT0010 (https://doi.org/10.54499/CEECIND/03501/2017/CP1420/CT0010)]; L.F.R. and M.J.S., grant numbers UIDB/04423/2020 and UIDP/04423/2020.

Institutional Review Board Statement: Not applicable. Animals were purchased dead.

Informed Consent Statement: Not applicable.

Conflicts of Interest: The authors declare no conflicts of interest.

References

1. Kent, M.L.; Andree, K.B.; Bartholomew, J.L.; El-Matbouli, M.; Desser, S.S.; Devlin, R.H.; Feist, S.W.; Hedrick, R.P.; Hoffmann, R.W.; Khattra, J.; Hallett, S.L.; Lester, R.J.; Longshaw, M.; Palenzuela, O.; Siddall, M.E.; Xiao, C. Recent advances in our knowledge of the Myxozoa. *J. Eukaryot. Microbiol.* **2001**, *48*, 395–413.
2. Lom, J.; Dyková, I. Myxozoan genera: definition and notes on taxonomy, life-cycle terminology and pathogenic species. *Folia Parasitol.* **2006**, *53*, 1–36.
3. Eszterbauer, E.; Atkinson, S.; Diamant, A.; Morris, D.; El-Matbouli, M.; Hartikainen, H. Myxozoan life cycles: practical approaches and insights. In Myxozoan Evolution, Ecology and Development, Okamura, B., Gruhl, A., Bartholomew, J.L. Eds.; Springer International Publishing, 2015; pp. 175–198.
4. Yokoyama, H.; Grabner, D.S.; Shirakashi, S. Transmission Biology of the Myxozoa. In Health and Environment in Aquaculture, Carvalho, E., David, G.S., Silva, R.J. Eds.; IntechOpen, 2012; pp. 3–42.
5. Fiala, I.; Bartošová-Sojková, P.; Whipps, C.M. Classification and phylogenetics of Myxozoa. In Myxozoan Evolution, Ecology and Development, Okamura, B., Gruhl, A., Bartholomew, J.L. Eds.; Springer International Publishing, 2015; pp. 85–110.
6. Okamura, B.; Hartigan, A.; Naldoni, J. Extensive Uncharted Biodiversity: The Parasite Dimension. *Integr. Comp. Biol.* **2018**, *58*, 1132–1145.

 doi:10.20944/preprints202506.0728.v1

7. Fiala, I. The phylogeny of Myxosporea (Myxozoa) based on small subunit ribosomal RNA gene analysis. *Int. J. Parasitol.* **2006**, *36*, 1521–1534.
8. Fiala, I.; Bartošová, P. History of myxozoan character evolution on the basis of rDNA and EF-2 data. *BMC Evol. Biol.* **2010**, *10*, 228.
9. Fiala, I.; Hlavničková, M.; Kodádková, A.; Freeman, M.A.; Bartošová-Sojková, P.; Atkinson, S.D. Evolutionary origin of *Ceratonova shasta* and phylogeny of the marine myxosporean lineage. *Mol. Phylogenet. Evol.* **2015**, *86*, 75–89.
10. Liu, Y.; Lövy, A.; Gu, Z.; Fiala, I. Phylogeny of Myxobolidae (Myxozoa) and the evolution of myxospore appendages in the *Myxobolus* clade. *Int. J. Parasitol.* **2019**, 49, 523–530.
11. Bartošová, P.; Fiala, I.; Jirků, M.; Cinková, M.; Caffara, M.; Fioravanti, M.L.; Atkinson, S.D.; Bartholomew, J.L.; Holzer, A.S. *Sphaerospora sensu stricto*: taxonomy, diversity and evolution of a unique lineage of myxosporeans (Myxozoa). *Mol. Phylogenet. Evol.* **2013**, *68*, 93–105.
12. Whipps, C.M.; Grossel, G.; Adlard, R.D.; Yokoyama, H.; Bryant, M.S.; Munday, B.L.; Kent, M.L. Phylogeny of the multivalvulidae (Myxozoa : Myxosporea) based on comparative ribosomal DNA sequence analysis. *J. Parasitol.* **2004**, *90*, 618–622.
13. Lom, J.; Noble, E.R. Revised classification of the class Myxosporea Butschli, 1881. *Folia Parasitol.* **1984**, *31*, 193–205.
14. Kent, M.L.; Moser, M. *Ortholinea alata* n. sp. (Myxosporea, Ortholineidae) in the Northern Butterfly fish *Chaetodon rainfordi*. *J. Protozool.* **1990**, *37*, 49–51.
15. Zhao, Y.; Song, W. *Myxoproteus cheni* sp n. and *Sinuolinea mai* sp n. (Myxosporea: Sinuolineidae) parasitic in the urinary bladder of marine fish (*Thamnaconus septentrionalis* Gunther, 1877) from the Yellow Sea, off the Qingdao coast of China. *Acta Protozool.* **2001**, *40*, 125–130.
16. Kovaleva, A.A.; Zubchenko, A.V.; Krasin, V.K. Foundation of a new Myxosporidean family (Protozoa, Myxosporidia) with a description of two new genera. *Parazitologiya* **1983**, *17*, 195–202.
17. Kodádková, A.; Bartošová-Sojková, P.; Holzer, A.S.; Fiala, I. *Bipteria vetusta* n. sp. – an old parasite in an old host: tracing the origin of myxosporean parasitism in vertebrates. *Int. J. Parasitol.* **2015**, *45*, 269–276.
18. Kovaleva, A.A.; Velev, P.; Vladev, P. New data on myxosporidians (Cnidospora: Myxosporea) fauna from commercial fishes of the Atlantic coast of Africa. In Ecology and resources of commercial fishes of the eastern Atlantic, Bukatin, P.A. Ed.; AtlantNIRO, Kaliningrad, 1993; pp. 174–193.
19. Kovaleva, A.A.; Rodjuk, G.N. New members of Myxosporidia (Cnidospora, Myxosporea) from fishes in the Falkland-Patagonian region. *Parazitologiya* **1991**, *25*, 549–551.
20. Sirin, C.; Santos, M.J.; Rangel, L.F. Morphological and molecular analyses of *Bipteria lusitanica* n. sp. in wild white seabream, *Diplodus sargus* (Linnaeus, 1758) in Portugal. *Parasitol. Res.* **2018**, *117*, 2035–2041.
21. Kalavati, C.; Anuradha, I. A new myxosporean, *Bipteria indica* sp. n. (Myxospora: Sinuolineidae) from the gall bladder of the striped mullet, *Mugil cephalus* Linneaus. *Acta Protozool.* **1995**, *34*, 307–309.
22. Geoffroy St. Hilaire, E. Poissons du Nil, de la mer Rouge et de la Méditerranée. In Description de l'Egypte ou recueil des observations et des recherches qui ont été faites en Égypte pendant l'expedition de l'Armée français, publié par les ordres de sa Majesté-L'Empereur Napoléon le Grand., Vol. 1; Histoire Naturelle, 1817; pp. 18–27.
23. FishStat: Global capture production 1950-2022. Available online: www.fao.org/fishery/en/statistics/software/fishstatj (accessed on 18 March 2025).
24. FishStat: Global aquaculture production 1950-2022. Available online: www.fao.org/fishery/en/statistics/software/fishstatj (accessed on 18 March 2025).
25. Alama-Bermejo, G.; Raga, J.A.; Holzer, A.S. Host-parasite relationship of *Ceratomyxa puntazzi* n. sp. (Myxozoa: Myxosporea) and sharpsnout seabream *Diplodus puntazzo* (Walbaum, 1792) from the Mediterranean with first data on ceratomyxid host specificity in sparids. *Vet. Parasitol.* **2011**, *182*, 181–192.
26. Athanasopoulou, F.; Prapas, T.; Rodger, H. Diseases of *Puntazzo puntazzo* Cuvier in marine aquaculture systems in Greece. *J. Fish Dis.* **1999**, *22*, 215–218.
27. Golomazou, E.; Athanassopoulou, F.; Karagouni, E.; Tsagozis, P.; Tsantilas, H.; Vagianou, S. Experimental transmission of *Enteromyxum leei* Diamant, Lom and Dyková, 1994 in sharpsnout sea bream, *Diplodus puntazzo* C. and the effect on some innate immune parameters. *Aquaculture* **2006**, *260*, 44–53.

 doi:10.20944/preprints202506.0728.v1

28. Lubat, J.; Radujkovic, B.; Marques, A.; Bouix, G. Parasites des poissons marins du Montenegro: Myxosporidies. *Acta Adriat.* **1989**, *30*, 31–50.
29. Katharios, P.; Garaffo, M.; Sarter, K.; Athanasopoulou, F.; Mylonas, C. A case of high mortality due to heavy infestation of *Ceratomyxa diplodae* in sharpsnout sea bream (*Diplodus puntazzo*) treated with reproductive steroids. *Bull. Eur. Assoc. Fish Pathol.* **2007**, *27*, 43–47.
30. Merella, P.; Cherchi, S.; Salati, F.; Garippa, G. Parasitological survey of sharpsnout seabream *Diplodus puntazzo* (Cetti, 1777) reared in sea cages in Sardinia (western Mediterranean). *Bull. Eur. Assoc. Fish Pathol.* **2005**, *25*, 140–147.
31. Rocha, S.; Casal, G.; Rangel, L.; Severino, R.; Castro, R.; Azevedo, C.; Santos, M.J. Ultrastructural and phylogenetic description of *Zschokkella auratis* sp. nov. (Myxozoa), a parasite of the gilthead seabream *Sparus aurata*. *Dis. Aquat. Org.* **2013**, *107*, 19–30.
32. Rocha, S.; Filipe Rangel, L.; Casal, G.; Severino, R.; Soares, F.; Rodrigues, P.; Santos, M.J. Occurrence of two myxosporean parasites in the gall bladder of white seabream *Diplodus sargus* (L.) (Teleostei, Sparidae), with the morphological and molecular description of *Ceratomyxa sargus* n. sp. *PeerJ* **2023**, *11*, e14599.
33. Lom, J.; Arthur, J.R. A guideline for the preparation of species descriptions in Myxosporea. *J. Fish Dis.* **1989**, *12*, 151–156.
34. Barta, J.R.; Martin, D.S.; Liberator, P.A.; Dashkevicz, M.; Anderson, J.W.; Feighner, S.D. Phylogenetic relationships among eight *Eimeria* species infecting domestic fowl inferred using complete small subunit ribosomal DNA sequences. *J. Parasitol.* **1997**, *83*, 262–271.
35. Hillis, D.M.; Dixon, M.T. Ribosomal DNA: molecular evolution and phylogenetic inference. *Q. Rev. Biol.* **1991**, *66*, 411–453.
36. Hallett, S.L.; Diamant, A. Ultrastructure and small-subunit ribosomal DNA sequence of *Henneguya lesteri* n. sp. (Myxosporea), a parasite of sand whiting *Sillago analis* (Sillaginidae) from the coast of Queensland, Australia. *Dis. Aquat. Org.* **2001**, *46*, 197–212.
37. Kent, M.L.; Khattra, J.; Hedrick, R.P.; Devlin, R.H. *Tetracapsula renicola* n. sp. (Myxozoa: Saccosporidae); the PKX myxozoan – the cause of proliferative kidney disease of salmonid fishes. *J. Parasitol.* **2000**, *86*, 103–111.
38. Whipps, C.M.; Adlard, R.D.; Bryant, M.S.; Lester, R.J.; Findlay, V.; Kent, M.L. First report of three *Kudoa* species from eastern Australia: *Kudoa thyrsites* from mahi mahi (*Coryphaena hippurus*), *Kudoa amamiensis* and *Kudoa minithyrsites* n. sp. from sweeper (*Pempheris ypsilychnus*). *J. Eukaryot. Microbiol.* **2003**, *50*, 215–219.
39. Werle, E.; Schneider, C.; Renner, M.; Völker, M.; Fiehn, W. Convenient single-step, one tube purification of PCR products for direct sequencing. *Nucleic Acids Res.* **1994**, *22*, 4354–4355.
40. Tamura, K.; Stecher, G.; Kumar, S. MEGA11: Molecular Evolutionary Genetics Analysis Version 11. *Mol. Biol. Evol.* **2021**, *38*, 3022–3027.
41. Katoh, K.; Rozewicki, J.; Yamada, K.D. MAFFT online service: multiple sequence alignment, interactive sequence choice and visualization. *Brief. Bioinform.* **2019**, *20*, 1160–1166.
42. Dereeper, A.; Guignon, V.; Blanc, G.; Audic, S.; Buffet, S.; Chevenet, F.; Dufayard, J.F.; Guindon, S.; Lefort, V.; Lescot, M.; Claverie, J.M.; Gascuell, O. Phylogeny.fr: robust phylogenetic analysis for the non-specialist. *Nucleic Acids Res.* **2008**, *36*, W465–W469.
43. Castresana, J. Selection of Conserved Blocks from Multiple Alignments for Their Use in Phylogenetic Analysis. *Mol. Biol. Evol.* **2000**, *17*, 540–552.
44. Guindon, S.; Dufayard, J.F.; Lefort, V.; Anisimova, M.; Hordijk, W.; Gascuel, O. New Algorithms and Methods to Estimate Maximum-Likelihood Phylogenies: Assessing the Performance of PhyML 3.0. *Syst. Biol.* **2010**, *59*, 307–321.
45. Ronquist, F.; Huelsenbeck, J.P. MrBayes 3: Bayesian phylogenetic inference under mixed models. *Bioinformatics* **2003**, *19*, 1572–1574.
46. Kuiter, R.H. Guide to Sea Fishes of Australia; New Holland Publishers, 2023; pp. 433.
47. Bauchot, M.L.; Hureau, J.C. Sparidae. In Check-list of the Fishes of the Eastern Tropical Atlantic (CLOFETA), Quero, J.C., Hureau, J.C., Karrer, C., Post, A., Saldanha, L. Eds.; Vol. 2; JNICT, Lisbon; SEI, Paris; and UNESCO, Paris, 1990.

 doi:10.20944/preprints202506.0728.v1

48. Fiala, I.; Bartošová-Sojková, P.; Okamura, B.; Hartikainen, H. Adaptive Radiation and Evolution Within the Myxozoa. In Myxozoan Evolution, Ecology and Development, Okamura, B., Gruhl, A., Bartholomew, J.L. Eds.; Springer International Publishing, 2015; pp. 69–84.
49. Bartošová, P.; Fiala, I.; Hypša, V. Concatenated SSU and LSU rDNA data confirm the main evolutionary trends within myxosporeans (Myxozoa: Myxosporea) and provide an effective tool for their molecular phylogenetics. *Mol. Phylogenet. Evol.* **2009**, *53*, 81–93.
50. Gunter, N.; Adlard, R. The demise of *Leptotheca* Thélohan, 1895 (Myxozoa: Myxosporea: Ceratomyxidae) and assignment of its species to *Ceratomyxa* Thélohan, 1892 (Myxosporea: Ceratomyxidae), *Ellipsomyxa* Koie, 2003 (Myxosporea: Ceratomyxidae), *Myxobolus* Bütschli, 1882 and *Sphaerospora* Thélohan, 1892 (Myxosporea: Sphaerosporidae). *Syst. Parasitol.* **2010**, *75*, 81–104.
51. Whipps, C.M. Interrenal disease in bluegills (*Lepomis macrochirus*) caused by a new genus and species of Myxozoan. *J. Parasitol.* **2011**, *97*, 1159–1165.
52. Atkinson, S.D.; Foott, J.S.; Bartholomew, J.L. Erection of *Ceratonova* n. gen. (Myxosporea: Ceratomyxidae) to encompass freshwater species *C. gasterostea* n. sp. from threespine stickleback (*Gasterosteus aculeatus*) and *C. shasta* n. comb. from salmonid fishes. *J. Parasitol.* **2014**, *100*, 640–645.
53. Freeman, M.A.; Kristmundsson, A. Studies of *Myxidium giardi* Cépède, 1906 infections in Icelandic eels identifies a genetically diverse clade of myxosporeans that represents the *Paramyxidium* n. g. (Myxosporea: Myxidiidae). *Parasit. Vectors* **2018**, *11*, 551.
54. Lom, J.; Dyková, I. New species of the genera *Zschokkella* and *Ortholinea* (Myxozoa) from the Southeast Asian teleost fish, *Tetraodon fluviatilis*. *Folia Parasitol.* **1995**, *42*, 161–168.
55. Guo, Q.; Huang, M.; Liu, Y.; Zhang, X.; Gu, Z. Morphological plasticity in *Myxobolus* Bütschli, 1882: a taxonomic dilemma case and renaming of a parasite species of the common carp. *Parasit. Vectors* **2018**, *11*, 399.
56. Zhai, Y.; Whipps, C.M.; Gu, Z.; Guo, Q.; Wu, Z.; Wang, H.; Liu, Y. Intraspecific morphometric variation in myxosporeans. *Folia Parasitol.* **2016**, *63*, 011.
57. Karlsbakk, E.; Kristmundsson, A.; Albano, M.; Brown, P.; Freeman, M.A. Redescription and phylogenetic position of *Myxobolus aeglefini* and *Myxobolus platessae* n. comb. (Myxosporea), parasites in the cartilage of some North Atlantic marine fishes, with notes on the phylogeny and classification of the Platysporina. *Parasitol. Int.* **2017**, *66*, 952–959.
58. Rocha, S.; Rocha, F.; Casal, G.; Mendonca, I.; Oliveira, E.; Al-Quraishy, S.; Azevedo, C. Supplemental diagnosis and phylogeny of *Myxobolus absonus* (Cnidaria, Myxozoa) from the eye of the freshwater fish *Pimelodus maculatus* (Siluriformes, Pimelodidae). *Acta Trop.* **2019**, *191*, 87–97.
59. Rocha, S.; Azevedo, C.; Oliveira, E.; Alves, A.; Antunes, C.; Rodrigues, P.; Casal, G. Phylogeny and comprehensive revision of mugiliform-infecting myxobolids (Myxozoa, Myxobolidae), with the morphological and molecular redescription of the cryptic species *Myxobolus exiguus*. *Parasitology* **2019**, *146*, 479–496.
60. Alama-Bermejo, G.; Jirků, M.; Kodádková, A.; Pecková, H.; Fiala, I.; Holzer, A.S. Species complexes and phylogenetic lineages of *Hoferellus* (Myxozoa, Cnidaria) including revision of the genus: A problematic case for taxonomy. *Parasit. Vectors* **2016**, *9*, 1–21.
61. Alama-Bermejo, G.; Viozzi, G.P.; Waicheim, M.A.; Flores, V.R.; Atkinson, S.D. Host-parasite relationship of *Ortholinea lauquen* sp. nov. (Cnidaria: Myxozoa) and the fish *Galaxias maculatus* in northwestern Patagonia, Argentina. *Dis. Aquat. Org.* **2019**, *136*, 163–174.
62. Chandran, A.; Zacharia, P.U.; Sanil, N.K. *Ortholinea scatophagi* (Myxosporea: Ortholineidae), a novel myxosporean infecting the spotted scat, *Scatophagus argus* (Linnaeus 1766) from southwest coast of India. *Parasitol. Int.* **2020**, *75*, 102020.
63. Shin, S.P.; Jin, C.N.; Sohn, H.; Kim, J.; Lee, J. *Ortholinea nupchi* n. sp. (Myxosporea: Ortholineidae) from the urinary bladder of the cultured olive flounder *Paralichthys olivaceus*, South Korea. *Parasitol. Int.* **2023**, *94*, 102734.

 doi:10.20944/preprints202506.0728.v1

64. Rangel, L.F.; Rocha, S.; Casal, G.; Castro, R.; Severino, R.; Azevedo, C.; Cavaleiro, F.; Santos, M.J. Life cycle inference and phylogeny of *Ortholinea labracis* n. sp. (Myxosporea: Ortholineidae), a parasite of the European seabass *Dicentrarchus labrax* (Teleostei: Moronidae), in a Portuguese fish farm. *J. Fish Dis.* **2017**, *40*, 243–262.
65. Lisnerová, M.; Martinek, I.N.; Alama-Bermejo, G.; Bouberlová, K.; Schaeffner, B.C.; Nkabi, N.; Holzer, A.S.; Bartošová-Sojková, P. An ancient alliance: Matching evolutionary patterns of cartilaginous fishes (Elasmobranchii) and chloromyxid parasites (Myxozoa). *Infect. Genet. Evol.* **2022**, *103*, 105346.
66. Holzer, A.S.; Bartošová-Sojková, P.; Born-Torrijos, A.; Lovy, A.; Hartigan, A.; Fiala, I. The joint evolution of the Myxozoa and their alternate hosts: A cnidarian recipe for success and vast biodiversity. *Mol. Ecol.* **2018**, *27*, 1651–1666.
67. Lisnerová, M.; Fiala, I.; Cantatore, D.; Irigoitia, M.; Timi, J.; Pecková, H.; Bartošová-Sojková, P.; Sandoval, C.M.; Luer, C.; Morris, J.; Holzer, A.S. Mechanisms and Drivers for the Establishment of Life Cycle Complexity in Myxozoan Parasites. *Biology* **2020**, *9*, 10.
68. Kodádková, A.; Dyková, I.; Tyml, T.; Ditrich, O.; Fiala, I. Myxozoa in high Arctic: Survey on the central part of Svalbard archipelago. *Int. J. Parasitol. Parasites Wildl.* **2014**, *3*, 41–56.
69. Rocha, S.; Casal, G.; Rangel, L.; Castro, R.; Severino, R.; Azevedo, C.; Santos, M.J. Ultrastructure and phylogeny of *Ceratomyxa auratae* n. sp. (Myxosporea: Ceratomyxidae), a parasite infecting the gilthead seabream *Sparus aurata* (Teleostei: Sparidae). *Parasitol. Int.* **2015**, *64*, 305–313.